Soil-atmosphere exchange of carbonyl sulfide in Mediterranean citrus orchard

Fulin Yang[1,2], Rafat Qubaja[1], Fyodor Tatarinov[1], Rafael Stern[1], and Dan Yakir[1,*]

1. Earth and Planetary Sciences, Weizmann Institute of Science, Rehovot 76100, Israel

2. College of Animal Sciences, Fujian Agriculture and Forestry University, Fuzhou 350002, China

***Correspondence:** Dan Yakir; email: dan.yakir@weizmann.ac.il

Abstract:

Carbonyl sulfide (COS) is used as a as a tracer of CO_2 exchange at the ecosystem and larger scales. The robustness of this approach depends on knowledge of the soil contribution to the ecosystem fluxes, which is uncertain at present. We assessed the spatial and temporal variations of soil COS and CO_2 fluxes in the Mediterranean citrus orchard combining surface flux chambers and soil concentration gradients. The spatial heterogeneity in soil COS exchange indicated net uptake below and between trees of up to 4.6 pmol m^{-2} s^{-1}, and net emission in sun exposed soil between rows, of up to 2.6 pmol m^{-2} s^{-1}, with overall mean uptake value of 1.1 ± 0.1 pmol m^{-2} s^{-1}. Soil COS concentrations decreased with soil depth from atmospheric levels of ~450 to ~100 ppt at 20 cm depth, while CO_2 concentrations increased from ~400 to ~5000 ppm. COS flux estimates from the soil concentration gradients were, on average, -1.0 ± 0.3 pmol m^{-2} s^{-1}, consistent with the chamber measurements. A soil COS flux algorithm driven by soil moisture and temperature (5 cm depth) and distance from the nearest tree, could explain 75% of variance in soil COS flux. Soil relative uptake, the normalized ratio of COS to CO_2 fluxes was, on average -0.4 ± 0.3 and showed a general exponential response to soil temperature. The results indicated that soil COS fluxes at our study site were dominated by uptake, with relatively small net fluxes compared to both soil respiration and reported canopy COS fluxes. Such result should facilitate the application of COS as a powerful tracer of ecosystem CO_2 exchange.

Keywords:

Carbonyl sulfide; COS; OCS; soil gas exchange; ecosystem gas exchange; tracer of carbon fluxes.

1. Introduction

Carbonyl sulfide (COS) is a Sulphur-containing analogue of CO_2 that is taken up by vegetation following a similar pathway to CO_2, ultimately hydrolyzed in an irreversible reaction with carbonic anhydrase. It therefore holds great promise for studies of photosynthetic CO_2 uptake (Asaf et al., 2013; Berry et al., 2013; Wehr et al., 2017; Whelan et al., 2018). One of the difficulties in the application of COS as a tracer for photosynthetic CO_2 uptake is that the non-leaf contributions to the net ecosystem COS flux are poorly characterized. There are reports of substantial soil fluxes, indicating both uptake and emissions (Kesselmeier et al., 1999; Kuhn et al., 1999; Masaki et al., 2016; Seibt et al., 2006; Yang et al., 2018; Yi et al., 2007). Although soil COS exchanges were in some cases small compared to plant uptake (e.g., Yang et al., 2018; Berkelhammer et al., 2014), this was not always the case. Substantial soil COS emissions have been found in wetlands and anoxic soils (Li et al., 2006; Whelan et al., 2013), and in senescing agricultural fields and high temperatures (Liu et al., 2010; Maseyk et al., 2014), or under drought conditions and in response to UV radiation (Kitz et al., 2017). Even for the same soil, COS fluxes could show large variations and both uptake and emission with sensitivities to soil moisture, and ambient COS concentrations (Bunk et al., 2017; Kaisermann et al., 2018). These studies also assessed the response of COS exchange to environmental controls, e.g. soil moisture and temperature and solar radiation.

For COS application as a tracer of ecosystem CO_2 exchange characterizing the relationships between COS and CO_2 fluxes is important. This is done by assessing the 'relative uptake' (RU) of the COS/CO_2 flux rate ratio, normalized by the ambient atmospheric concentrations (that differ for the two gases by a factor of about 10^6), as done at the leaf scale, (LRU) or ecosystem scale (ERU; e,g, Asaf et al., 2013). It was similarly applied to soil as SRU (Berkelhammer et al., 2014). Conservative, or predictable, SRU values reflect systematic relationships between the processes influencing CO_2 and COS, could help the identification of the dominant process, and support the application of COS as tracer. Small SRU values compared to LRU could also indicate reduced effect of soil on ecosystem fluxes. For example, Berkelhammer

et al. (2014) reported mean SRU of -0.76, which are about half of the leaf values of about +1.7 indicating that compared to CO_2, leaf COS is enhanced, and soil COS uptake is suppressed, which provides additional robustness to the COS-GPP approach. Note also that as soil CO_2 flux measurements and modeling are much more common than for COS at flux sites. Knowledge of SRU could help derive soil COS fluxes and, for example, improve the partitioning of canopy COS flux from NEE_{COS} measurements.

Soil COS exchange has often been measured by incubations in the lab (e.g., Bunk et al., 2017; Kesselmeier et al., 1999; Liu et al., 2010; Van Diest and Kesselmeier, 2008), and by static or dynamic chambers in the field (e.g., Berkelhammer et al., 2014; Kitz et al., 2017; Sun et al., 2018; Yi et al., 2007; Mseyk et al., 2014), and using models (e.g., Ogée et al., 2016; Sun et al., 2015; Whelan et al., 2016). In spite of these efforts, more field measurements of soil COS exchange are clearly needed as a basis for elucidating underlying mechanism, as well as obtaining better quantitative record of the possible range of soil COS fluxes under natural conditions. Note also that previous studies have focused on agricultural soils (Maseyk et al., 2014), wetlands (Whelan et al., 2013), boreal forest soils (Sun et al., 2018), and grasslands (Kitz et al., 2017), but several ecosystems are understudied, such as in the Mediterranean. Finally, soil profile measurements will also be useful for validation of soil models of COS exchange (Sun et al., 2015). The objective of this study was to apply dynamic chambers measurements, constrained by simultaneous soil gradient method to assess the spatial and temporal variations soil COS and CO_2 fluxes in a citrus orchard ecosystem where contrasting soil microsite conditions occur.

2. Materials and methods

2.1 Field site

The study was conducted in an orchard in Rehovot, Israel (31°54′ N, 34°49′ E, 50 m, asl) in 2015 and 2016. The orchard is a plantation of lemon trees (*Citrus limonia Osbeck*), with 5 m distance between rows and 4 m between trees. Mean annual air temperature at the site is 19.7 °C, and mean annual precipitation is 537 mm. Most of the precipitation (82%) falls in November to February with no rain during June to

October. A trickle irrigation system was used from May to September with the standard irrigation plan of the orchard management. The soil in the area is brown red sandy soil (hamra soil) with an average bulk density of 1.6 kg m^{-3} and pH of 6.5 (Singer, 2007). Although root distribution was not measured we noted that roots were concentrated mainly within about 50 cm of the tree trunks, as could be expected due to drip irrigation installed around the trunk.

2.2 Quantum cascade laser measurements

We used the commercially available quantum cascade laser (QCL) system (Aerodyne Research, Billerica, MA) with tunable laser absorption spectrometer (Model: QC-TILDAS-CS) to measure COS, CO_2, and water vapor concentrations simultaneously. The device was installed in a mobile lab, described by Asaf et al. (2013). COS is detected at 2050.40 cm^{-1} and CO_2 at 2050.57 cm^{-1} at a rate of 1 Hz. The instrument was calibrated using working reference compressed air tank that was used for inter-comparison with the NOAA GMD lab (Boulder CO). Corrections for water vapor were made using the TDLWINTEL software installed in the QCL (Kooijmans et al. 2016)

2.3 Soil chamber flux measurements

Custom-made stainless-steel cylindrical chamber of 177 cm^2 directly inserted into the soil (~5 cm) was used, as previously described (Berkelhammer et al., 2014; Yang et al., 2018). The chambers were opaque and photoproduction was not considerate in this study. The chamber air and ambient air flows were pumped to the QCL analyzer through two 3/8-inch diameter Decabon tubing. Flow rate was maintained at 1.2 L min^{-1} and repeatedly cycled with 1 min instrument background (using N_2 zero gas), 9 min ambient air flow, and 10 min chamber air sample. Three different soil sites were used with distance of 3.20, 2.00 and 0.25 m away from a tree trunk, that represented sampling sites between rows (BR), between trees (BT) and under tree (UT). Each sampling site was measured continuously for 24 hours and cycled between sites for the duration of the campaign. Four measurement campaigns were carried out during 5th~9th August

2015; 25th~28th December 2015; 5th~9th May 2016; 28th~31th July 2016.

Gas exchange rates, F_c, were calculated according to:

$$F_c = \frac{Q}{A} \times \left(\Delta C_{sample} - \Delta C_{blank} \right) \qquad (1)$$

where Q is the chamber flush rate in mol s^{-1}; A is the enclosed soil surface in m^2; ΔC is the gas concentrations difference between chamber air and ambient air in pmol mol^{-1} for COS and μmol mol^{-1} for CO_2 under sampling, and blank reference treatments (using the same chamber placed above a sheet of aluminum foil before and after measurement at each site. Hereafter, the soil fluxes are reported in pmol m^{-2} s^{-1} and μmol m^{-2} s^{-1} for COS and CO_2, respectively. Soil relative uptake (SRU) is used to characterize the relationship between soil CO_2 and COS fluxes, was estimated from the normalized ratio of CO_2 respiration to COS uptake (negative values) or emission (positive values) fluxes (Berkelhammer et al., 2014):

$$SRU = \frac{F_{COS_{soil}}}{[COS]} \Big/ \frac{F_{CO_{2soil}}}{[CO_2]} \qquad (2)$$

2.4 Soil concentration profile measurements

Four campaigns of soil concentration profile measurements were carried out during 1st~2nd March; 20th~26th April; 10th May; 22nd~28th June of 2016. The trace gas at five soil depths of 0, 2.5, 5.0, 10, 20 cm was sampled at each of the three microsites, BR, BT and UT.

Four individual Decabon tubes were inserted at adjacent but different points into the soil (to avoid communication between tubes during sampling), to the different depths indicated above and connected directly to the QCL positioned close by the mobile lab. At least one day after insertion and insuring sealing between tubing and soil, soil air was sampled with flow rate of 80 ml min^{-1}, in a 10 min cycle of 1 min instrument background, 3 min surface air (depth 0; used initially to flush all above ground tubing), 5 min sampling of a depth point in the profile (first two minutes for flushing the tubing, third minute used for data; up to 400 ml extracted from the soil), ending with 1 min surface air. Five complete sets of cycles including the four soil depths and surface air

were repeated for each site (with time gaps between cycles of hours, and in some cases overnight). The pressure in the 500 ml QCL sample cell was kept at 15 torr to insure sufficient turnovers (~8 per minute using the low flow rate) before data were recorded.

Assuming that in the selected measurement sites, soil trace gas is only transported by diffusion, soil COS and CO_2 fluxes were estimated based on the Fick's first law:

$$F = -D_s \frac{dC}{dz_{soil}} \qquad (3)$$

where F is the upward or downward gas flux (pmol m^{-2} s^{-1} for COS and μmol m^{-2} s^{-1} for CO_2); D_s is the effective gas diffusion coefficient of the relevant gas species in the soil (m^2 s^{-1}); C the trace gas concentration (mixing ratio, converted from the measured mole fractions); z_{soil} is the soil depth (m).

The Penman (1940) function was used to describe the soil diffusion coefficient (D_s) as in Kapiluto et al. (2007):

$$D_s = D_a\left(\theta_s - \theta\right)\sqrt{\frac{T_s + 273.15}{298.15}} \qquad (4)$$

where θ_s is the soil saturation water content and θ is the measured soil volumetric water content. D_a is the trace gas diffusion coefficient in free air, which varied with temperature and pressure, given by

$$D_a = D_{a0}\left(\frac{T_s + 273.15}{293.15}\right)^{1.75}\left(\frac{P}{101.3}\right) \qquad (5)$$

where D_{a0} is a reference value of trace gas diffusion coefficient at 293.15 K and 101.3 kPa, given as 1.24×10^{-5} m^{-2} s^{-1} for COS (Seibt et al., 2010) and 1.47×10^{-5} m^{-2} s^{-1} for CO_2 (Jones, 1992); T_s is soil temperature (°C), and P is air pressure (kPa).

3. Results

3.1 Variations in soil COS flux

Soil COS fluxes showed significant heterogeneity at both the spatial (microsites) and temporal (seasonal) scale (Fig. 1). Overall, the hourly soil COS flux varied from -4.6 to +2.6 pmol m^{-2} s^{-1}, with mean value of 1.1 ± 0.1 pmol m^{-2} s^{-1}. On the spatial scale,

the COS fluxes showed systematically uptake under trees (UT), moderate uptake and some emissions between trees (BT) and relatively more emission in the exposed area between rows (BR), with diurnal mean values across seasons of -3.0 ± 0.1, -0.4 ± 0.1 and +0.1 ± 0.1 pmol m^{-2} s^{-1}, respectively.

On the diurnal time-scale, soil COS flux were generally higher in the afternoon (peaking around 15:00~16:00 hours), declining at night and early morning (Fig. 1). On the seasonal time scale, soil COS fluxes showed both changes in rates and shifts from net uptake to net emission, with the site hierarchy differing in the different seasons (Fig. 1). In the UT site where only COS uptake was observed, the highest rates were observed in winter and peak summer (December and Auguest) with diurnal mean rates of nearly -4 pmol m^{-2} s^{-1}, and more moderate uptake rates, around -2 pmol m^{-2} s^{-1}, in spring and early summer (May and July; Fig. 1). In the BT sites, significant COS uptake of ~-2.5 pmol m^{-2} s^{-1} was observed in winter, but net fluxes were near zero in other times, with some afternoon emission in summer. In the exposed BR sites, minor uptake (less than -1 pmol m^{-2} s^{-1}) was observed in spring and early summer, but consistent emission in peak summer, with diurnal mean values of nearly +2 pmol m^{-2} s^{-1}.

3.2 Effects of moisture and temperature

During the hot summer (August 2015 and July 2016), differences in microsite soil water content (θ) were most distinct, with θ of nearly 30% in the UT sites (associated with drip irrigation), but ~19% and ~12% in the BT and BR sites. Correspondingly, the UT sites had significant COS uptake of about -3 pmol m^{-2} s^{-1} while the other sites showed emission of about +1 pmol m^{-2} s^{-1} (Table 1). In winter (December), θ in the three sites was similar, ~25%, and all sites showed soil COS uptake, but with clear gradient of -3.9, -2.5 and -0.7 pmol m^{-2} s^{-1} in the UT, BT and BR sites, respectively (Fig. 1). On average, soil COS fluxes showed non-linear increase in uptake with increasing θ, but it seems that this response may saturate at about θ of 25% and uptake rates of ~-3.9 pmol m^{-2} s^{-1} (Fig. 2). The fit to the data presented in Fig. 2 also indicate that in dry soil with θ<15% soil COS emission can be expected.

The response of soil COS fluxes to soil temperature varied among the three

measurement sites (Fig. 3). The BT and BR sites showed a near linear response with a shift from uptake to emisson around 25 °C. In the shaded and moist UT site, COS uptake was always significant ranging between -4 to -1 pmol m^{-1} s^{-1} with relatively low temperature sensitivity, and with lowest mean uptake rates around 20 °C.

Pearson product-moment correlation analysis results showed that hourly soil COS flux was significantly related to soil moisture and temperature (at the 0.001 level), and the soil moisture had a stronger environmental controls on the soil COS flux (r=-0.77), compared with soil temperature (r=+0.45).

Comprehensive assessment of the effects of soil moisture (θ), temperature (T_s) and distance away from tree trunk (d), showed that hourly soil COS flux (F_{COS}) could be fitted to a three parameters exponential model, which could explain 75% of the variation in soil COS flux (Eq. 6).

$$F_{COS} = 8.91\exp(0.01T_s - 0.01\theta + 0.09d - 0.33) - 8.86,\ R^2 = 0.75 \qquad (6)$$

3.3 COS flux estimates from soil concentration gradients

The average soil concentration gradient of COS and CO_2 for the four campaigns is shown in Fig. 4. COS concentrations decreased with soil depth, with the opposite trend for CO_2, consistent with the results reported above of soil surface COS uptake and CO_2 emission at our orchard site. COS concentrations at depth of 2.5 cm was on average 314 ppt, and about one-third lower than the mean surface, ambient, value of 460 ppt. The lowest COS concentration at depth of 20 cm (166 ppt) was almost one-third of that at the soil surface. An exponential and a linear equations provided reasonable fit to the changes in soil COS and CO_2 concentrations, respectively, as a function of depth (z_{soil}):

$$\begin{aligned} [COS] &= 283.5\exp\left(-0.2z_{soil}\right) + 169.9,\ R^2 = 0.99 \\ [CO_2] &= 122.2z_{soil} + 558.5,\ R^2 = 0.99 \end{aligned} \qquad (7)$$

In terms of individual site and campaign, all profiles except for BR in summer (June) showed the general trend of decreasing [COS] and increasing [CO_2] with depth, with the steepest gradient at the top 5 cm (Fig. 5). In the BR microsite in summer, CO_2

profiles were shallow, consistent with the low respiration (see July BR in Table 1). But a decrease in COS concentration toward the surface, with surface value lower than the next two soil depth points (Fig. 5J), was consistent with COS emission at that time (July BR in Table 1).

As noted above, the profile data generally exhibited the steepest gradient at the top few cm of the soil, indicating that the dominating COS sink (and likely also the CO_2 source) was located at shallow depth. We therefore used the gas concentration difference at two shallowest depths (z_{soil1} = 0 and z_{soil2} = 2.5 cm) to provide an approximation of the fluxes to and from the soil, to constrain the more extensive chamber measurements. The COS diffusion coefficient, D_s, was estimated for each campaigns (see Methods), indicating low D_s value in the UT site in June and July (D_s = 2.55 $mm^2\ s^{-1}$), associated with the drip irrigation and the high soil water content, and high values in the dryer soils (D_s = 5.57 $mm^2\ s^{-1}$), with an average COS diffusion coefficient of 4.4 ± 0.3 $mm^2\ s^{-1}$. The soil COS flux estimates using the gradient method is reported in Table 2. COS flux varied between -2.1 to +1.6 pmol $m^{-2}\ s^{-1}$ with a mean value of -1.0 ± 0.3 pmol $m^{-2}\ s^{-1}$ during the measurement periods, consistent with the mean value of 1.1 ± 0.1 pmol $m^{-2}\ s^{-1}$ reported above for the chamber measurements. Also in agreement with the chamber measurements, fluxes at UT and BT always showed COS uptake, with generally higher values in spring (March) than in summer (May-June), while the BR data indicated change from uptake in spring (March-April, -1.3 to -1.6 pmol $m^{-2}\ s^{-1}$) to emission in June (+1.6 pmol $m^{-2}\ s^{-1}$).

3.4 Soil relative uptake

Soil was always a source of CO_2 due respiration (combined autotrophic and heterotrophic respiration). Soil CO_2 flux rates varied both spatially and temporally in similar patterns to those of COS, and with overall range of +0.3 to +14.6 μmol $m^{-2}\ s^{-1}$ (Table 1). The highest soil respiration values were observed in the UT sites in summer (July, August; Table 1), with intermediate (+1 to about +3 μmol $m^{-2}\ s^{-1}$) and low values (< +1 μmol $m^{-2}\ s^{-1}$) in the BT and BR sites, respectively. Generally, soil COS exchange

varied from release to increasing uptake with increasing CO_2 production in a non-linear way (Fig. 6a). The normalized ratio of COS to CO_2 fluxes (SRU; Eq. 2) varied from -1.9 to +1.9 with an average value of -0.4 ± 0.3, with negative values indicating COS uptake linked to CO_2 emission. SRU values showed response to both soil temperature (Fig. 6b) and soil moisture (Fig. 6c), although with relatively low R^2 values. Respiration increased with temperature while COS uptake declined and at temperature above about 25 °C SRU turned positive when both COS and CO_2 are emitted from the soil. SRU exhibited inverse relationships with soil moisture, with positive values in dry soil and increasingly negative values with increasing soil moisture (Fig. 6c). Based on its combined temperature (T_s) and moisture (θ) response, SRU could be forecasted by the following algorithm, which explained 67% of the observed variations (Eq. 8):

$$SRU = 0.01\exp(0.17T_s) - 0.02\theta - 1.00,\ R^2 = 0.67 \qquad (8)$$

ANOVA analysis results indicated that SRU was not significantly different among the three observation microsites (BR, BT, and UT; $P > 0.05$). Between the seasonal campaigns, however, SRU values peaked in summer (+0.5 ± 0.7) with highest averaged soil temperature (29 °C) and was significantly higher than winter SRU (-1.4 ± 0.6) when soil temperature was lowest (11 °C; $P < 0.05$), and with no significant difference in SRU among the other campaigns ($P > 0.05$).

4. Discussions

4.1 Heterogeneity in soil COS exchange

The observed soil-atmosphere COS exchange rates observed in this study (both mean and range; Fig. 1, Table 1) are consistent with values reported in a range of other ecosystems (-1.4 to -4.9 pmol m^{-2} s^{-1}; Steinbacher et al., 2004; Kitz et al., 2017; White et al., 2010; Berkelhammer et al., 2014), but lower than -11.0 to -11.8 pmol m^{-2} s^{-1} in a riparian and subtropical forests (Berkelhammer et al., 2014; Yi et al., 2007). Soil COS emissions were also observed in summer and spring campaigns, with maximal COS emission consistent with the values of +1.8 to +2.6 pmol m^{-2} s^{-1} observed in a riparian and alpine forests (Berkelhammer et al., 2014), but significantly lower than reported in

298 the senescing agricultural ecosystem (~+30 pmol $m^{-2}s^{-1}$; Maseyk et al., 2014).

299 The observed range in the soil-atmosphere exchange fluxes reflected significant
300 heterogeneity on both the spatial and the temporal scales. The spatial scale
301 heterogeneity clearly reflected the contrasting microsite conditions with lower
302 temperatures and higher moisture under the trees (UT sites), compared with the higher
303 temperatures and lower moisture in exposed soil between rows (BR sites), with
304 intermediate, partially shaded, conditions between trees (BT sites). Indeed, a large
305 fraction of the variations in the COS flux (~75%) could be explained by a simple
306 algorithm as a function of these two variables, temperature and moisture. Note that
307 while temperature and θ co-varied in general, with high temperatures associated with
308 drier soil, under the wet UT conditions, sensitivity to temperature was significantly
309 reduced. In the dry soil conditions, emission was associated with high temperature, and
310 in the BR sites also with high solar radiation. However, all measurements were made
311 in dark chambers and could not involve photochemical production, which was also
312 demonstrated in agricultural soil by Kitz et al. (2017). Apparently even under dark
313 conditions, high temperature can induce high emission rates, as also noted when the
314 thermal insolation on the soil chamber in the BR site was incidentally removed and a
315 large spike in temperature (52 ºC) and emission of 11.4 pmol m^{-2} s^{-1} was observed. Note
316 also that the soil profile resuts indicated that the emission source was below surface,
317 and maybe non-photochemical irrespective of the chamber opaquenes.

318 Temporal variations were observed both on the daily and seasonal time scales.
319 Diurnal changes were, however, minor compared to the changes from winter to summer
320 in all microsites. Shifts from uptake to emission were observed essentially only on the
321 seasonal time scale (Fig. 1). This likely reflected the dominance of soil moisture on the
322 COS flux rates. This is because θ did not change noticeably on the daily scale, while it
323 did changed considerably across seasons (between 10.0 and 35.5% overall). Soil
324 temperatures did change over the daily cycle (e.g. 26.0 to 42.4 ºC in the BR site during
325 summer), although such changes are still smaller than the seasonal changes in soil
326 temperature (e.g. 10.5 to 31.8 ºC in the BR site). A dominant role of soil moisture in
327 explaining the variations in COS uptake is consistent with the results of Van Diest and

Kesselmeier (2008), but less so with the negligible θ effects in grassland under simulated drought (Kitz et al., 2017).

COS uptake is thought to be related to carbonic anhydrase activity in soil (Kesselmeier et al., 1999), which could be via microorganisms (Piazzetta et al., 2015), such as Bacteria (Kamezaki et al., 2016; Kato et al., 2008), or fungi (Bunk et al., 2017; Li et al., 2010; Masaki et al., 2016). CA activity is also influenced by soil moisture (Davidson and Janssens, 2006; Seibt et al., 2006), although soil moisture can also directly influence soil gas diffusion rates (Ogée et al., 2016; Sun et al., 2015). The effect of CA on COS exchange can also be related to root distribution and the effects of CA activity within plant roots (Seibt et al., 2006; Viktor and Cramer, 2005; Whelan and Rhew, 2015). This could influence the spatial variations and soil moisture effects on COS exchange in this study as most of the roots were distributed around the restricted trees' drip irrigation zone at UT sites, and was sparse in the dryer areas, such as the BR and BT sites (un-quantified observations).

At least part of the variations in soil COS fluxes could also reflect the differential effects of environmental conditions on COS uptake and production process (Ogée et al., 2016). Solubility in soil water (with COS solubility of 0.8 ml ml^{-1}; Svoronos and Bruno, 2002) could also be significant, especially in the UT microsites, influenced by the drip irrigation from May to September that could involve water percolation to deeper soil layers. The drivers of soil COS production are still unclear. COS could be produced by chemical processes in the lab (Ferm, 1957), but can also be produced by biotic process in soils such as by hydrolysis of metallic thiocyanates (Katayama et al., 1992) with thiocyanate hydrolase (Conrad, 1996; Svoronos and Bruno, 2002) and hydrolysis of CS_2 (Cox et al., 2013; Smith and Kelly, 1988). Fungi are also reported to be the source of COS (Masaki et al., 2016). Additionally, abiotic thermal degradation of organic matter leading to COS production may be consistent with the temperature sensitivity of COS emission in the BR microsite where biotic processes can be expected to be minimized. Similar high temperature-dependent soil COS emissions were reported in midlatitude forest (Commane et al., 2015) and agricultural field (Maseyk et al., 2014). Lab incubation results also indicated thermal production of COS in soil with increasing

temperature (Liu et al., 2010; Whelan et al., 2016; Whelan and Rhew, 2015). Photochemical production of soil COS was also proposed (Sun et al., 2015; Whelan and Rhew, 2015), and assumed to be driven by ultraviolet fraction of incoming solar radiation (Kitz et al., 2017). Note, however, that all measurements in the present study were made in the dark. In addition, the chemical reaction of CO and $MgSO_4$ under heating could also produce COS (Ferm, 1957). Note that $MgSO_4$ has been reported in our study soil (Singer, 2007), and we observed relatively high CO concentration in our field site (not shown due to insufficient calibration). Finally, the balance between the uptake (likely biotic dominated) and emission (likely abiotically dominated) can also be influenced by soil nitrogen (Kaisermann et al., 2018).

4.2 Soil relative uptake

We use SRU values to assess the relative importance of the soil COS flux compared with the canopy, and indicate shifts from conservative links between processes influencing COS and CO_2 (see Introduction). On average, the value of SRU at our site was smaller than reported for riparian or pine forests (-0.37 vs -0.76 and -1.08; Berkelhammer et al., 2014; Sun et al., 2018). This may reflect the contribution of COS emissions at BR and BT in summer, that were not observed in the forest study. Overall, the mean SRU values observed here indicated that the soil COS uptake flux was proportionally less than 40% of the soil respiration flux. In contrast with the canopy fluxes where the COS uptake flux is, proportionally, nearly twice as large as the CO_2 assimilation flux (LRU~1.6 at our site; Yang et al., 2018; 1.7 across vegetation types, Whelan et al., 2018). In contrast to leaves with robust LRU value that tend toward a constant, SRU at our site varied between -1.9 and +1.9. However, this range was observed only in the dryer and exposed BR sites, while in the shaded and moist UT sites, it was much narrower, -0.1 to -0.8. Furthermore, it seems that the high SRU values (both positive and negative) represented conditions where the actual fluxes were small (COS uptake was on average -3.0 in the UT but only 0.1 pmol m^{-2} s^{-1} in the BR sites. It seems that the large SRU values in the BR microsites, were also associated with low

soil respiration, 0.5 μmol m^{-2} s^{-1} in BR sites, compared to 10 μmol m^{-2} s^{-1} in the UT sites. It is therefore possible that the low SRU values are the more significant for ecosystem scale studies and indicate a much smaller contribution to overall ecosystem fluxes than that of the canopy (i.e., SRU~-0.4 vs LRU~+1.7).

Differential effects of changing environmental conditions on production and uptake processes were reflected in relatively large spatial and temporal heterogeneity observed in the soil COS exchange at our site. However, the contrasting effects of production and emission may explain both the sharp increase in SRU values at high temperatures as the effects of production counteract uptake (Fig. 6b), and the much lower sensitivity to temperature of COS flux compared to that of CO_2 (Fig. 6a). Such contrasting consumption/production effects may, in fact, reduce the magnitude of the net flux of soil COS, and may explain the relatively narrow range of SRU values.

Application of COS as a tracer for canopy CO_2 exchange requires the accounting for the soil effects and while knowledge of SRU can help predicting it, ultimately we need to quantify the fluxes. Note in that respect, that in our recent canopy scale study at the same site (Yang et al., 2018) indicated that in spite of the considerable variations in soil COS fluxes, the soil COS uptake fluxes were equivalent to ~1% of the daytime foliage flux across seasons, and reached ~3% in the spring peak season (but larger proportions were observed during more stressful periods when fluxes were overall small).

4.3 Soil COS profiles

Complementing our chamber measurements with soil profile measurements of COS and CO_2 concentrations provided constrain on the relatively new surface soil COS measurements and provided additional information on the possible location of the source/sink in the soil. Using the near surface gradient yielded flux estimates comparable to chamber measurements, providing a useful and rare quantitative validation. For example, in May, the chamber and profile measurements were made at about the same time (5th~9th May for chamber and 10th May for profile) and the

differences between chamber (all microsites) and gradient flux estimates, was negligible (~0.2-0.6 pmol m^{-2} s^{-1}). However, the profile results indicated in addition that the sink/source activities concentrated at top soil layers, probably at around 5-10 cm depth, as reflected in the minimum or maximum in gas concentrations (emphasizing the need for high vertical resolution in employing the profile approach). The variable profiles observed below these points must reflect temporal dynamics in the sink/source activities across the profile. The near surface peak activity makes it particularly sensitive to variations in temperature and moisture, as indeed observed (Figs. 2, 3). Low COS concentration in the lower parts of the profile may result from continuous removal of soil COS and may indicate distribution of CA activity beyond the litter layer and the soil surface (Seibt et al., 2006). COS production, however, seems to occur only near the soil surface with no indication for production in deeper layer, consistent with its high temperature sensitivity, and not necessarily dependent on radiation (e.g. Kitz et al., 2017).

Note that the gradient method based on the Fick's diffusion law have its own limitations (Kowalski and Sánchezcañete, 2010;Sánchez-Cañete et al., 2017;Bekele et al., 2007). However, it is simple low-cost approach and can help diagnose the magnitude of soil fluxes, which can also help in identifying below ground processes and their locations.

5. Conclusions

Our detailed analysis of the spatial and temporal variations in soil-atmosphere exchange of COS provided new information on a key uncertainty in the application of ecosystem COS flux to assess productivity. Furthermore, we provide validation of the surface chamber measurements that are generally in use, by the additional gradient approach. Our results show that both microsites and seasonal variations in COS fluxes were related to soil moisture, temperature, and the distance from the tree (likely reflecting root distribution), but we suggest that soil moisture is the predominant environmental control over soil COS exchanges at our site. A simple algorithm was sufficient to forecast most of the variations in soil COS flux supporting its incorporated

into ecosystem scale applications, as we recently demonstrated in a parallel study at the same site (Yang et al., 2018).

Clearly, uncertainties are still associated with soil processes involving COS, the differential effects of soil moisture, temperature, and communities of microorganisms and are likely to contribute to both the spatial and temporal variations in soil net COS exchange and require further research.

Author contributions:

DY designed the study; FY, RQ, FT, RS and DY performed the experiments. FY and FT analyzed the data. DY and FY wrote the paper with discussions and contributions to interpretations of the results from all co-authors.

Acknowledgements

We are grateful to Omri Garini, Madi Amer, and Boaz Ninyo-Setter for their help. This work was supported by the Minerva foundation, a joint NSFC-ISF grant 2579/16; Israel Science Foundation (ISF 1976/17), the German Research Foundation (DFG) as part of the CliFF Project, and the JNF-KKL. FY is supported by the National Natural Science Foundation of China (41775105), and the Natural Science Foundation of Gansu Province (17JR5RA341).

References

Asaf, D., Rotenberg, E., Tatarinov, F., Dicken, U., Montzka, S. A., and Yakir, D.: Ecosystem photosynthesis inferred from measurements of carbonyl sulphide flux, Nat. Geosci., 6, 186-190, 2013.

Bekele, A., Kellman, L., and Beltrami, H.: Soil Profile CO_2 concentrations in forested and clear cut sites in Nova Scotia, Canada, Forest. Ecol. Manag., 242, 587-597, 2007.

Berkelhammer, M., Asaf, D., Still, C., Montzka, S., Noone, D., Gupta, M., Provencal, R., Chen, H., and Yakir, D.: Constraining surface carbon fluxes using in situ measurements of carbonyl sulfide and carbon dioxide, Global Biogeochem. Cy., 28, 161-179, 2014.

Berry, J., Wolf, A., Campbell, J. E., Baker, I., Blake, N., Blake, D., Denning, A. S., Kawa, S. R., Montzka, S. A., and Seibt, U.: A coupled model of the global cycles of carbonyl sulfide and CO_2: A possible new window on the carbon cycle, J. Geophys. Res.:Biogeo., 118, 842-852, 2013.

Bunk, R., Behrendt, T., Yi, Z., Andreae, M. O., and Kesselmeier, J.: Exchange of carbonyl sulfide (OCS) between soils and atmosphere under various CO_2 concentrations, J. Geophys. Res.:Biogeo., 122, 1343-1358, 2017.

Commane, R., Meredith, L. K., Baker, I. T., Berry, J. A., Munger, J. W., Montzka, S. A., Templer, P. H., Juice, S. M., Zahniser, M. S., and Wofsy, S. C.: Seasonal fluxes of carbonyl sulfide in a midlatitude forest, P. Natl. Acad. Sci. U.S.A., 112, 14162-14167, 2015.

Conrad, R.: Soil microorganisms as controllers of atmospheric trace gases (H_2, CO, CH_4, OCS, N_2O, and NO), Microbiol. Rev., 60, 609-640, 1996.

Cox, S. F., McKinley, J. D., Ferguson, A. S., O'Sullivan, G., and Kalin, R. M.: Degradation of carbon disulphide (CS2) in soils and groundwater from a CS_2-contaminated site, Environ. Earth Sci., 68, 1935-1944, 2013.

Davidson, E. A., and Janssens, I. A.: Temperature sensitivity of soil carbon decomposition and feedbacks to climate change, Nature, 440, 165-173, 2006.

Ferm, R. J.: The chemistry of carbonyl sulfide, Chemical Reviews, 57, 621-640, 1957.

Jones H G . Plants and Microclimate: A Quantitative Approach to Environmental Plant Physiology, Cambridge University Press, 1983.

Kaisermann, A., Ogée, J., Sauze, J., Wohl, S., Jones, S. P., Gutierrez, A., and Wingate, L.: Disentangling the rates of carbonyl sulfide (COS) production and consumption and their dependency on soil properties across biomes and land use types, Atmos. Chem. Phys., 18, 9425-9440, 2018.

Kamezaki, K., Hattori, S., Ogawa, T., Toyoda, S., Kato, H., Katayama, Y., and Yoshida, N.: Sulfur Isotopic Fractionation of Carbonyl Sulfide during Degradation by Soil Bacteria, Environ. Sci. Technol., 50, 3537-3544, 2016.

Kapiluto, Y., Dan, Y., Tans, P., and Berkowitz, B.: Experimental and numerical studies of the ^{18}O exchange between CO_2 and water in the atmosphere–soil invasion flux, Geochim. Cosmochim. Ac., 71, 2657-2671, 2007.

Katayama, Y., Narahara, Y., Inoue, Y., Amano, F., Kanagawa, T., and Kuraishi, H.: A thiocyanate hydrolase of Thiobacillus thioparus. A novel enzyme catalyzing the formation of carbonyl sulfide from thiocyanate, J. Biol. Chem., 267, 9170-9175, 1992.

Kato, H., Saito, M., Nagahata, Y., and Katayama, Y.: Degradation of ambient carbonyl sulfide by Mycobacterium spp. in soil, Microbiology+. 154, 249-255, 2008.

Kesselmeier, J., Teusch, N., and Kuhn, U.: Controlling variables for the uptake of atmospheric carbonyl sulfide by soil, J. Geophys. Res.: Atmos., 104, 11577-11584, 1999.

Kitz, F., Gerdel, K., Hammerle, A., Laterza, T., Spielmann, F. M., and Wohlfahrt, G.: In situ soil COS exchange of a temperate mountain grassland under simulated drought, Oecologia, 183, 851-860, 2017.

Kooijmans L.M.J., Uitslag N.A.M., Zahnister M.S., Nelson D.D., Motzka S.A. and Chen H.: Continuous and high precision atmospheric concentration measurements of COS, CO_2, CO and H_2O using a quantum cascade laser spectrometer (QCLS). Atmos. Meas. Tech., 9, 5293-5314, 2016

Kowalski, A. S., and Sánchezcañete, E. P.: A New Definition of the Virtual Temperature, Valid for the Atmosphere and the CO_2-Rich Air of the Vadose Zone, J. Appl.

Meteorol. Clim., 49, 1238-1242, 2010.

Kuhn, U., Ammann, C., Wolf, A., Meixner, F., Andreae, M., and Kesselmeier, J.: Carbonyl sulfide exchange on an ecosystem scale: Soil represents a dominant sink for atmospheric COS, Atmos. Environ., 33, 995-1008, 1999.

Li, X., Liu, J., and Yang, J.: Variation of H_2S and COS emission fluxes from Calamagrostis angustifolia Wetlands in Sanjiang Plain, Northeast China, Atmos. Environ., 40, 6303-6312, 2006.

Li, X. S., Sato, T., Ooiwa, Y., Kusumi, A., Gu, J. D., and Katayama, Y.: Oxidation of elemental sulfur by Fusarium solani strain THIF01 harboring endobacterium Bradyrhizobium sp, Microb. Ecol., 60, 96-104, 2010.

Liu, J., Geng, C., Mu, Y., Zhang, Y., Xu, Z., and Wu, H.: Exchange of carbonyl sulfide (COS) between the atmosphere and various soils in China, Biogeosciences, 7, 753-762, 2010.

Masaki, Y., Ozawa, R., Kageyama, K., and Katayama, Y.: Degradation and emission of carbonyl sulfide, an atmospheric trace gas, by fungi isolated from forest soil, FEMS Microbiol. Lett., 363, fnw197, 2016.

Maseyk, K., Berry, J. A., Billesbach, D., Campbell, J. E., Torn, M. S., Zahniser, M., and Seibt, U.: Sources and sinks of carbonyl sulfide in an agricultural field in the Southern Great Plains, P. Natl. Acad. Sci. U.S.A., 111, 9064-9069, 2014.

Ogée, J., Sauze, J., Kesselmeier, J., Genty, B., Van Diest, H., Launois, T., and Wingate, L.: A new mechanistic framework to predict OCS fluxes from soils, Biogeosciences, 13, 2221-2240, 2016.

Penman, H. L.: Gas and Vapor Movements in the Soli: I. The diffusion of vapors through porous solids, J. Agric. Sci., 30, 437-462, 1940.

Piazzetta, P., Marino, T., and Russo, N.: The working mechanism of the beta-carbonic anhydrase degrading carbonyl sulphide (COSase): a theoretical study, Phys. Chem. Chem. Phys., 17, 14843-14848, 2015.

Sánchez-Cañete, E. P., Scott, R. L., Van Haren, J., and Barron-Gafford, G. A.: Improving the accuracy of the gradient method for determining soil carbon dioxide efflux, J. Geophys. Res.:Biogeo., 122, 2017.

554 Seibt, U., Kesselmeier, J., Sandoval-Soto, L., Kuhn, U., and Berry, J.: A kinetic analysis
555 of leaf uptake of COS and its relation to transpiration, photosynthesis and carbon
556 isotope fractionation, Biogeosciences, 7, 333-341, 2010.
557 Seibt, U., Wingate, L., Lloyd, J., and Berry, J. A.: Diurnally variable $\delta^{18}O$ signatures of
558 soil CO_2 fluxes indicate carbonic anhydrase activity in a forest soil, J. Geophys.
559 Res.: Atmos., 111, G04005, 2006.
560 Singer, A.: The soils of Israel, Springer Science & Business Media, 2007.
561 Smith, N. A., and Kelly, D. P.: Oxidation of carbon disulphide as the sole source of
562 energy for the autotrophic growth of Thiobacillus thioparus strain TK-m,
563 Microbiology+. 134, 3041-3048, 1988.
564 Steinbacher, M., Bingemer, H. G., and Schmidt, U.: Measurements of the exchange of
565 carbonyl sulfide (OCS) and carbon disulfide (CS_2) between soil and atmosphere
566 in a spruce forest in central Germany, Atmos. Environ., 38, 6043-6052, 2004.
567 Sun, W., Maseyk, K., Lett, C., and Seibt, U.: A soil diffusion–reaction model for surface
568 COS flux: COSSM v1, Geosci. Model. Dev., 8, 3055-3070, 2015.
569 Sun, W., Kooijmans, L. M. J., Maseyk, K., Chen, H., Mammarella, I., Vesala, T., Levula,
570 J., Keskinen, H., and Seibt, U.: Soil fluxes of carbonyl sulfide (COS), carbon
571 monoxide, and carbon dioxide in a boreal forest in southern Finland, Atmos. Chem.
572 Phys., 18, 1363-1378, 2018.
573 Svoronos, P. D., and Bruno, T. J.: Carbonyl sulfide: a review of its chemistry and
574 properties, Ind. Eng. Chem. Res., 41, 5321-5336, 2002.
575 Van Diest, H., and Kesselmeier, J.: Soil atmosphere exchange of carbonyl sulfide (COS)
576 regulated by diffusivity depending on water-filled pore space, Biogeosciences, 5,
577 475-483, 2008.
578 Viktor, A., and Cramer, M. D.: The influence of root assimilated inorganic carbon on
579 nitrogen acquisition/assimilation and carbon partitioning, New Phytol., 165, 157-
580 169, 2005.
581 Wehr, R., Commane, R., Munger, J. W., McManus, J. B., Nelson, D. D., Zahniser, M.
582 S., Saleska, S. R., and Wofsy, S. C.: Dynamics of canopy stomatal conductance,
583 transpiration, and evaporation in a temperate deciduous forest, validated by

carbonyl sulfide uptake, Biogeosciences, 14, 389, 2017.

Whelan, M. E., Min, D.-H., and Rhew, R. C.: Salt marsh vegetation as a carbonyl sulfide (COS) source to the atmosphere, Atmos. Environ., 73, 131-137, 2013.

Whelan, M. E., and Rhew, R. C.: Carbonyl sulfide produced by abiotic thermal and photodegradation of soil organic matter from wheat field substrate, J. Geophys. Res.:Biogeo., 120, 54-62, 2015.

Whelan, M. E., Hilton, T. W., Berry, J. A., Berkelhammer, M., Desai, A. R., and Campbell, J. E.: Carbonyl sulfide exchange in soils for better estimates of ecosystem carbon uptake, Atmos. Chem. Phys., 16, 3711-3726, 2016.

Whelan, M. E., Lennartz, S. T., Gimeno, T. E., Wehr, R., Wohlfahrt, G., Wang, Y., Kooijmans, L. M. J., Hilton, T. W., Belviso, S., Peylin, P., Commane, R., Sun, W., Chen, H., Kuai, L., Mammarella, I., Maseyk, K., Berkelhammer, M., Li, K. F., Yakir, D., Zumkehr, A., Katayama, Y., Ogée, J., Spielmann, F. M., Kitz, F., Rastogi, B., Kesselmeier, J., Marshall, J., Erkkilä, K. M., Wingate, L., Meredith, L. K., He, W., Bunk, R., Launois, T., Vesala, T., Schmidt, J. A., Fichot, C. G., Seibt, U., Saleska, S., Saltzman, E. S., Montzka, S. A., Berry, J. A., and Campbell, J. E.: Reviews and syntheses: Carbonyl sulfide as a multi-scale tracer for carbon and water cycles, Biogeosciences, 15, 3625-3657, 2018.

White, M., Zhou, Y., Russo, R., Mao, H., Talbot, R., Varner, R., and Sive, B.: Carbonyl sulfide exchange in a temperate loblolly pine forest grown under ambient and elevated CO_2, Atmos. Chem. Phys., 10, 547-561, 2010.

Yang, F., Qubaja, R., Tatarinov, F., Rotenberg, E., and Yakir, D.: Assessing canopy performance using carbonyl sulfide measurements, Glob. Change Biol., 24, 3486-3498, 2018.

Yi, Z., Wang, X., Sheng, G., Zhang, D., Zhou, G., and Fu, J.: Soil uptake of carbonyl sulfide in subtropical forests with different successional stages in south China, J. Geophys. Res.: Atmos., 112, D08302, 2007.

Figure captions:

Figure 1. Spatial variability of soil COS flux at three sites, between trees (a), between rows (b), and under tree (c). Each figure shows the diurnal cycling of soil COS flux in the four campaigns. Each data point was the hourly mean ± 1 S.E. (N=3).

Figure 2. Relationship of soil COS flux and soil moisture. Each data point represents the diurnal average (n=24) for each microsite and season (measurement campaign). Error bars represent ±1 S.E. around the mean; errors for flux are about the size of the symbols.

Figure 3. Soil COS fluxe as a function of temperature and its linear regression line. Each data point represents the diurnal average (n=24) for each site and season (campaign). Error bars represent ±1 S.E. around the mean.The data point marked in black cirble were collected during irrigation cycle (enhanced uptake) and were excluded from the regression.

Figure 4. Mean COS and CO_2 concentrations at different soil depth. The COS concentration decreases exponentially with soil depth. The data point is the mean of the combined data at each of the four measurement campaigns (N=4; ± 1 S.E.).

Figure 5. Soil COS and CO_2 concentration profiles at the three microsites in four measurement campaigns**.** The data points are the mean of all measurements in a campaign (N=4, ± 1 S.E.)

Figure 6. The relationships between soil COS and CO_2 flux rates (chamber measurements; a). The response of soil relative uptake (SRU; normalized ratio of COS to CO_2 fluxes) to soil temperature (b) and to soil water content (c). The data points represent the diurnal average (N=24) of each site and season (measurement campaign). Error bars represent ± 1 S.E. around the mean (often the size of the symbol).

635 **Table 1.** Mean values of soil COS and CO_2 flux rates across sites (BR, between rows;
636 BT, between trees; UT, under tree), and seasons, together with the normalized ratio of
637 COS/CO_2 fluxes (SRU), and the mean soil temperature at 5 cm depth (T_s) and soil water
638 content (% by wt; θ).

Campaigns	Sites	COS flux (pmol m^{-2} s^{-1})	CO_2 flux (μmol m^{-2} s^{-1})	SRU	T_s (°C)	θ (%)
August, 2015	BR	1.83±0.08	0.77±0.04	1.85	31.66±1.01	9.98±0.28
	BT	0.06±0.05	3.33±0.05	0.01	29.09±0.20	19.77±0.02
	UT	-3.64±0.13	10.79±0.12	-0.26	28.80±0.26	24.03±0.40
December, 2015	BR	-0.74±0.07	0.30±0.02	-1.92	10.50±0.17	23.33±1.89
	BT	-2.52±0.10	1.21±0.03	-1.62	11.20±0.19	24.22±0.94
	UT	-3.87±0.08	3.81±0.07	-0.79	12.17±0.16	26.11±1.01
May, 2016	BR	-0.77±0.02	0.32±0.02	-1.88	21.67±0.32	15.56±0.38
	BT	-0.05±0.04	1.31±0.05	-0.03	22.20±0.34	15.70±1.03
	UT	-1.80±0.11	10.78±0.54	-0.13	20.35±0.38	22.11±1.44
July, 2016	BR	0.21±0.04	0.79±0.05	0.21	29.66±0.60	14.73±0.57
	BT	0.76±0.09	1.97±0.04	0.30	26.68±0.15	17.49±0.70
	UT	-2.67±0.09	14.58±0.40	-0.14	27.83±0.34	35.47±3.47

639

Table 2. Estimates of soil COS and CO_2 fluxes from soil concentration gradient measurements (T_s, soil temperature; θ, soil water content; BR, between rows; BT, between trees; UT, under tree.)

Campaigns	Sites	COS flux (pmol m^{-2} s^{-1})	CO_2 flux (μmol m^{-2} s^{-1})	CO_2 diffusion coefficient (mm^2 s^{-1})	COS diffusion coefficient (mm^2 s^{-1})	T_s (°C)	θ (%)
March, 2016	BR	-1.31	2.34	5.21	4.40	17.9	19.4
	BT	-1.15	2.21	4.80	4.05	16.2	21.8
	UT	-2.10	5.89	4.76	4.02	17.3	22.4
April, 2016	BR	-1.55	1.07	6.66	5.62	23.0	11.0
	BT	-0.89	1.14	6.44	5.43	20.4	11.6
	UT	-1.74	4.73	6.01	5.07	22.4	15.2
May, 2016	BR	-0.98	2.21	5.68	4.79	21.9	17.4
	BT	-0.51	1.24	5.06	4.27	22.0	21.6
	UT	-1.20	11.36	3.11	2.63	20.1	34.5
June, 2016	BR	1.55	2.63	6.61	5.57	35.9	15.5
	BT	-1.17	2.60	5.20	4.39	26.3	21.7
	UT	-1.19	11.85	3.02	2.55	22.9	35.6

Figure 1

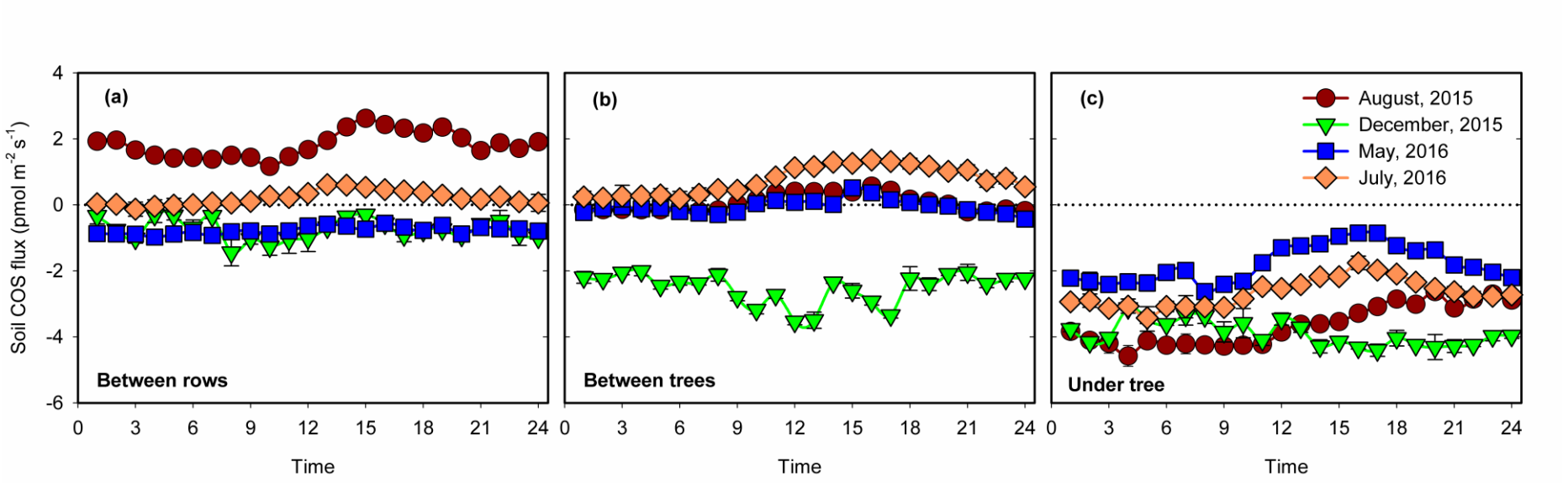
(a)
(b)
(c)
Between rows
Between trees
Under tree
Soil COS flux (pmol m-2 s-1)
Time
August, 2015
December, 2015
May, 2016
July, 2016

Figure 2

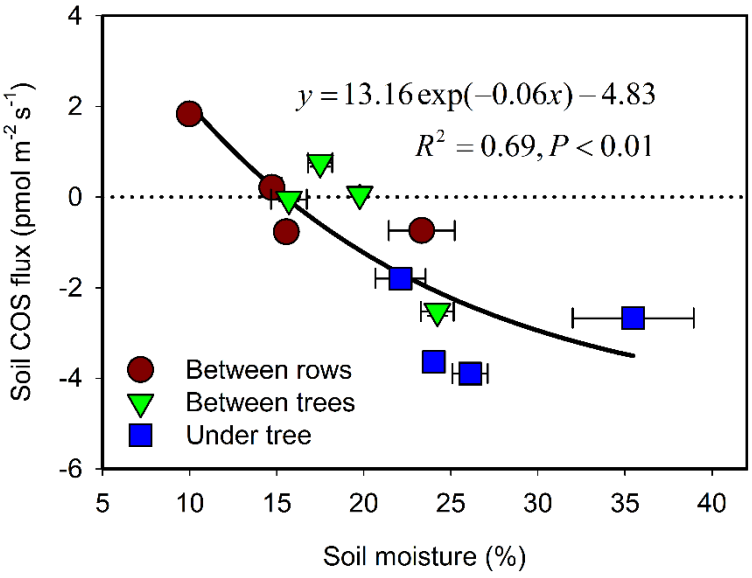
$y = 13.16\exp(-0.06x) - 4.83$
$R^2 = 0.69, P < 0.01$
Between rows
Between trees
Under tree
Soil COS flux (pmol m^{-2} s^{-1})
Soil moisture (%)
4
2
0
-2
-4
-6
5
10
15
20
25
30
35
40

Figure 3

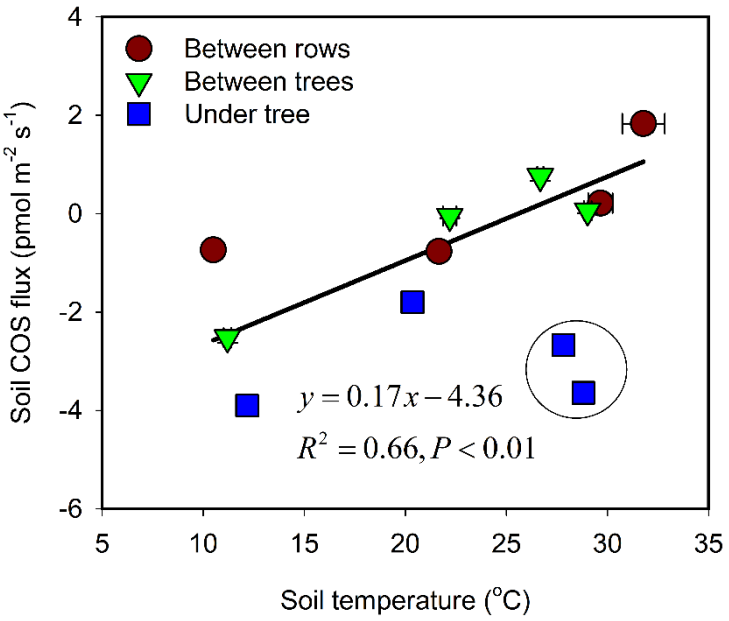
Between rows
Between trees
Under tree
$y = 0.17x - 4.36$
$R^2 = 0.66, P < 0.01$
Soil COS flux (pmol m^{-2} s^{-1})
Soil temperature (°C)
4
2
0
-2
-4
-6
5
10
15
20
25
30
35

Figure 4

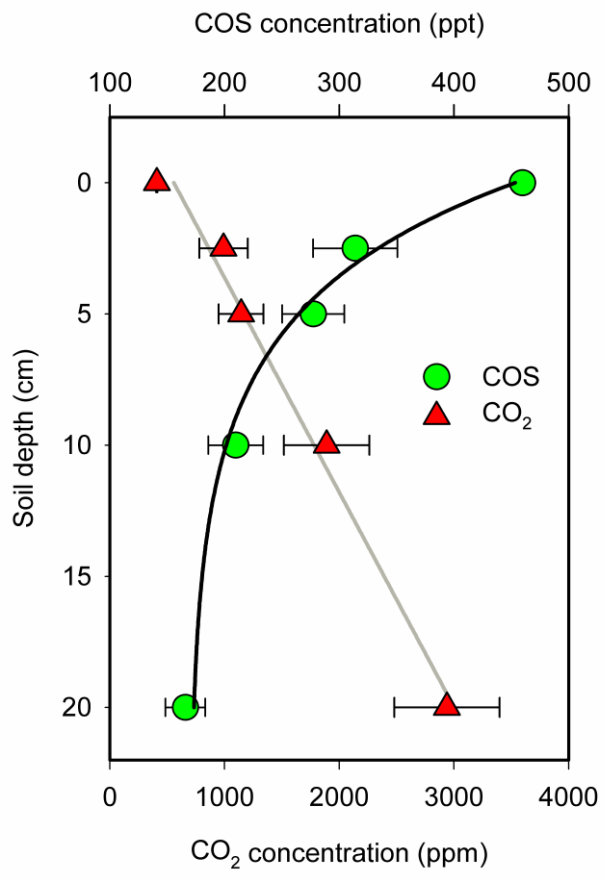
COS concentration (ppt)
100
200
300
400
500
0
5
10
15
20
Soil depth (cm)
COS
CO2
0
1000
2000
3000
4000
CO2 concentration (ppm)

Figure 5

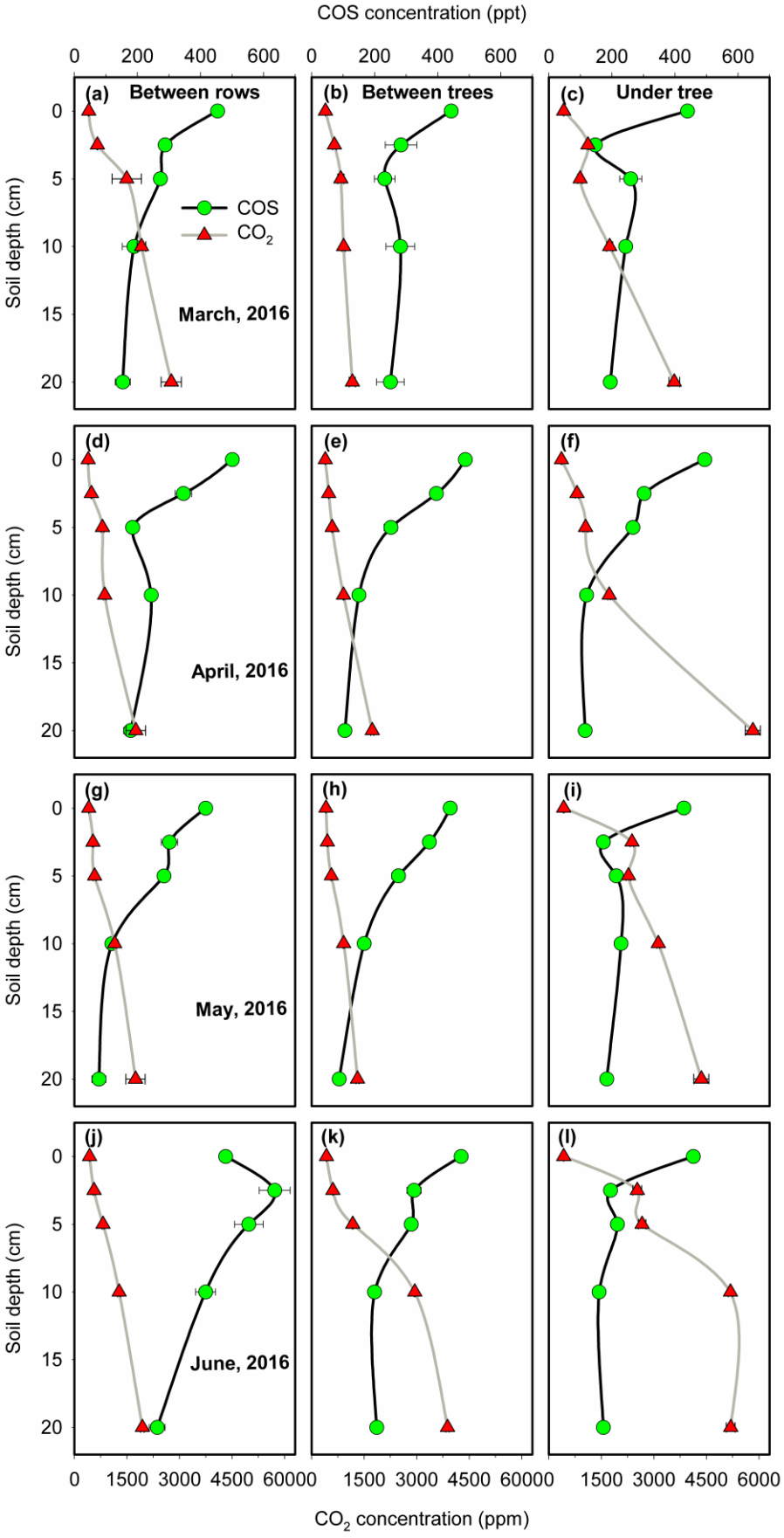
COS concentration (ppt)
0 200 400 600
(a) Between rows
(b) Between trees
(c) Under tree
COS
CO2
March, 2016
April, 2016
May, 2016
June, 2016
Soil depth (cm)
0 5 10 15 20
(d)
(e)
(f)
(g)
(h)
(i)
(j)
(k)
(l)
0 1500 3000 4500 60000
1500 3000 4500 60000
1500 3000 4500 6000
CO2 concentration (ppm)

Figure 6

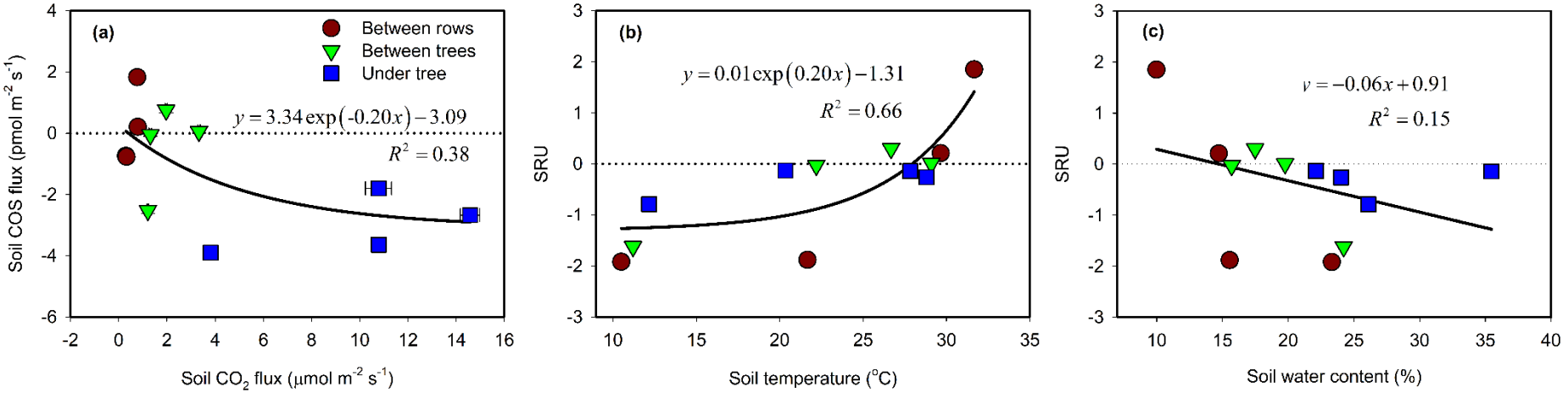
(a)
Between rows
Between trees
Under tree
$y = 3.34\exp(-0.20x) - 3.09$
$R^2 = 0.38$
Soil COS flux (pmol m^{-2} s^{-1})
Soil CO$_2$ flux (μmol m^{-2} s^{-1})
(b)
$y = 0.01\exp(0.20x) - 1.31$
$R^2 = 0.66$
SRU
Soil temperature (°C)
(c)
$y = -0.06x + 0.91$
$R^2 = 0.15$
SRU
Soil water content (%)